FEATURE ARTICLE

Atomic Scale Friction and Different Phases of Motion of Embedded Molecular Systems

M. G. Rozman

Institut fur Polymere, ETH Zentrum, CH-8092 Zurich, Switzerland, and Institut of Physics, Tartu University, Riia 142, EE2400 Tartu, Estonia

M. Urbakh* and J. Klafter

School of Chemistry, Tel Aviv University, Tel Aviv 69978, Israel

F.-J. Elmer

Institut für Physik, Universitat Basel, CH-4056 Basel, Switzerland

Received: February 27, 1998; In Final Form: May 18, 1998

Interfacial friction is one of the oldest problems in physics and chemistry and certainly one of the most important from a practical point of view. Due to its practical importance and the relevance to basic scientific questions, there has been a major increase in the activity of the study of interfacial friction on the microscopic level during the last decade. New experimental tools have been developed that allow for detailed investigations of friction at nanometer length scales, a range of related processes which have been termed nanotribology. Intriguing structural and dynamical features have been observed experimentally in nanoscale molecular systems confined between two atomically smooth solid surfaces. These include, for example, stick−slip motion, intermittent stick−slip motion characterized by force fluctuations, transition to sliding above the critical velocity, and a dependence of friction on the history of the system. These and other observations have motivated theoretical efforts, both numerical and analytical, but most issues remain controversial. In spite of the recently growing efforts, many aspects of friction are still not well understood. In this feature article we investigate in detail a minimalistic model which includes most of the relevant microscopic parameters needed to obtain the above experimental observables. We also establish relationships between the properties of the embedded system and the frictional forces. Our aim is to better understand the origins of friction and to learn how to control its nature. Our approach leads to a new look at this old problem and to predictions amenable to experimental tests.

Introduction

The field of nanotribology evolves around the attempts to understand the relationship between frictional forces and the microscopic properties of systems. Recent revival of interest in friction[1−6] has unraveled a broad range of phenomena and new behaviors which help shed light on some "old" concepts which are already considered textbook material. These include the static and kinetic friction forces, transition to sliding, and thinning, which have been widely discussed but whose microscopic meaning is still lacking.

New experimental tools have been developed that allow for detailed investigations of confined molecules and macromolecules down to nanometer length scales. As an example, the surface forces apparatus (SFA) has been modified to explore shear forces between two atomically flat solid surfaces separated by molecularly thin liquid layers,[7−10] see Figure 1. Summarizing the experimental observations, one distinguishes between low driving velocity region ($v < v_c$), where the system exhibits solid-like behavior, and higher driving velocities ($v > v_c$) which correspond to a more liquid-like behavior. A sharp boundary at $v = v_c$ is observed between the solid-like and the liquid-like regimes. Figure 2 exhibits different types of frictional forces as observed experimentally.[11] As seen in the figure, the low velocity regime is characterized by a stick−slip motion which is basically determined by the static and kinetic friction forces and whose details depend on the mechanical properties of the

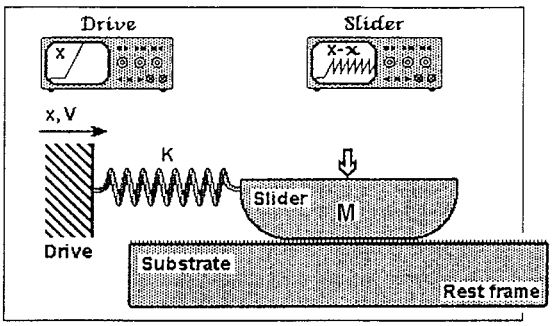

Figure 1. Basic tribological system (from ref 10).

* To whom correspondence should be addressed. Email: urbakh@post.tau.ac.il.

S1089-5647(98)01332-7 CCC: $15.00
Published on Web 09/19/1998

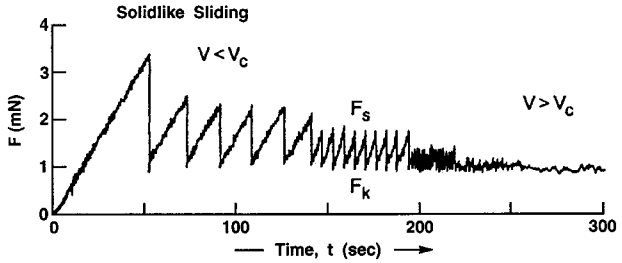

Figure 2. Typical friction traces for solidlike nanolayers; here shown for two close-packed DMPE monolayers sliding at 25 °C (ref 11). With solidlike monolayers stick−slip motion often occurs at low sliding velocities but reverts to smooth sliding above the critical velocity which is $v_c = 0.1$ μm/s in this case.

probing system. For high velocities, the system exhibits a smooth sliding motion which resembles a thinning of the effective viscosity. Typical of the intermediate range between low and high driving velocities is a chaotic behavior which is still to be investigated.

What one wishes to deduce from the above experimental observations are new insights that will help establish the basics of nanotribology, differentiate among different embedded systems, and enable one to control the desired type of motion. To be more specific: (i) Which of the observables depend on the properties of the *embedded molecular system* and which on the *mechanical setup?* (ii) How do the static (F_s) and kinetic (F_k) friction forces and the characteristic velocities, determining the transition to sliding, depend on the molecule−molecule and molecule−surface interactions? (iii) What is the effect of incommensurability of the liquid and solid structures on the frictional dynamics? (iv) What are the time and length scales that dictate the duration of slip events in the stick−slip motion, and how do they affect the critical velocity v_c corresponding to the transition from stick−slip to sliding? (v) What are the phases of the embedded molecular system that correspond to the different regimes of motion? (vi) What is hidden under the chaotic behavior and how to quantitatively analyze it? (vii) How does one extract the velocity dependent frictional forces from experimental data?

Some of these questions have been already addressed in previous works based mainly on large scale molecular dynamics calculations.[12−15] Atomistic molecular dynamics simulations have a wide range of applicability and have reached a high level of accuracy. They have however their inherent limitations. Right now, time scales of tens of nanoseconds and length scales of tens of nanometers are attainable in computer simulations. These time and length scales may not be sufficient for the consideration of slow relaxation processes in liquid films which play an important role in friction and lubrication phenomena. The time scale and length scale of the fluctuations in liquid films should increase drastically near points of phase transitions, which have been suggested[13,14] for the explanation of stick−slip motion. The origin of stick−slip motion and its related phenomena remains therefore still under some debate. Nevertheless, the limitation of time scales is not the principal problem of atomistic molecular dynamics simulations, as it will be hopefully resolved in the future. The basic open questions concerning molecular dynamics simulations relate to derivations of general laws which are not sensitive to the specific details of the simulations and the discovery of the few parameters controlling the processes under consideration.

In this feature article we would like to discuss above the questions within a minimalistic model which is still general enough and includes most of the parameters relevant to address

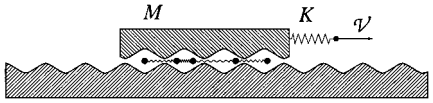

Figure 3. Schematic sketch of the model geometry.

the questions raised above (see Figure 3). The model serves as an example of how to establish the relationships between the microscopic characteristics and the macroscopically observed quantities. However, our conclusions, we believe, are mostly model independent.

Model

We use here the minimal number of parameters required to discuss the frictional properties of molecular systems embedded between two plates one of which is externally driven (Figure 3). We distinguish between the mechanical (external) parameters and the parameters of the embedded system (internal). The internal parameters in our model are m the mass of a single particle in the chain of N identical particles; U_0 the amplitude of the potential of period b that represents the corrugation of the molecule−plate interaction in the lateral direction; ω_{ch} the characteristic frequency that corresponds to the intrachain interactions; η the dissipation coefficient which is responsible for the dissipation of the kinetic energy of each particle, due to excitations in the plate; δ is the misfit between the substrate and chain periods, $\delta = (b - a)/b$, where a is the spatial period of undisturbed chain. There are two characteristic intrinsic frequencies in this model: ω_{ch} and $\omega = (2\pi/b)\sqrt{U_0/m}$ which is the frequency of the small oscillations of the particle in the minima of the particle−plate potential. The external parameters are M, the plate mass, and K the spring constant of the spring connecting the top plate to the stage. There is also an external frequency related to these parameters, $\Omega = \sqrt{K/M}$.

The model presented in Figure 3 leads to a number of different dynamical behaviors as the stage velocity is varied. We have observed four quantitatively different dynamical regimes;[16] (a) at low velocities we observe a stick−slip motion of the plate; (b) as the stage velocity increases the motion of the top plate is characterized by irregular stop events with time intervals between them that increase rapidly with v. Thus, the stick−slip motion becomes more erratic and intermittent (c) in the kinetic regime the top plate never stops and the spring executes chaotic oscillations, and (d) two types of smooth sliding occur when the stage velocity is above the critical velocity v_c. Similar behaviors are typically observed in experiments on thin sheared liquids and have recently been reported also for sheared granular layers.[17]

There are, generally, two approaches used to investigate shear forces of confined liquids: tribological (constant driving velocity)[7,9] and theological (oscillatory external drive).[8] In the bulk the two approaches lead to similar results, but less is known about the relationship between tribology and rheology in nanoscale confined systems. Here we concentrate on the tribological approach where the velocity is a well defined variable. Establishing a relationship between these approaches is essential for creating a unifying description of the response to shear.

Static and Kinetic Friction

Low driving velocity measurements lead to a distinction between two fundamental quantities: *static* (F_s) and *kinetic* (F_k) friction forces, which determine the behavior at early stages of the motion. F_s is the force needed to initiate the motion

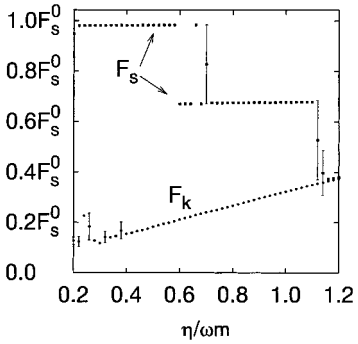

Figure 4. Static F_s and kinetic F_k friction forces as a function of the dissipation coefficient. The calculations were done for the following values of parameters: $v = 0.03b\omega$, $\epsilon = m/M = 1/120$, $N = 15$, $\delta = 0.05$, $\omega_{ch}/\omega = 1$, $\Omega/\omega = 0.015$. Error bars on the graph denote the dispersion of the averaged values of forces. The force unit F_s^0 is defined by eq 1: $F_s^0 = 2\pi U_0/b$.

(depinning force in our model). F_k is the minimal force necessary to keep the plate sliding. On the basis of the assumption that the system was in the ground state before initiating the motion, F_s is expressed by the amplitude of the potential corrugation and can be shown to be

$$F_s = F_s^0 = \frac{2\pi U_0}{b} \tag{1}$$

for noninteracting particles. It is clear from eq 1 that F_s depends on the internal parameters only.

When considering the kinetic friction, the dissipative nature of the system enters and F_k depends also on the external parameter M. F_k can be obtained by balancing the gain in energy due to the driving force and the energy loss due to dissipation. An estimate, again for noninteracting particles, leads to[18]

$$F_k = \frac{8}{\pi}\eta\sqrt{\frac{U_0}{M}} \tag{2}$$

Inferring F_s and F_k from experiments requires some caution. It is generally accepted[10] that in the overdamped case ($\eta^2 > 4KM$) the static and kinetic friction forces correspond to the maxima and minima in the spring force observed during stick−slip oscillations. However, this practical definition holds only if after each slip the system relaxes back to its ground state. Thus the experimentally obtained value of F_s may depend on the rate of equilibration prior to its measurements. Figure 4 presents an example where F_s is ill-defined since the condition for arriving back to the ground state is not fulfilled, and the system still carries the "memory" of the previous dynamical state. The kinetic friction in Figure 4 follows eq 2. The stick−slip behavior disappears when F_k approaches F_s.

In the underdamped limit ($\eta^2 < 4KM$) the temporal behavior of the slip part is dominated by the response time of the mechanical system $\sim 2\pi/\Omega$. Therefore, deducing F_k from the minima of the stick−slip regime might be misleading. We will come back to this point later. Because U_0 competes as well with the dissipation coefficient η and with the mechanical external parameters we have chosen to work in the limit $\eta^2 < 8\pi U_0 M/b$, which is underdamped with respect to η and U_0. This limit ensures the observation of macroscopic stick−slip.

Effective Frictional Force

The various experimental observations obtained by SFA measurements (stick−slip, transition to sliding, details of slip events, etc.) can be understood and analyzed in terms of an effective velocity dependent force that acts on the top plate. The slow motion of the top plate follows the following equation

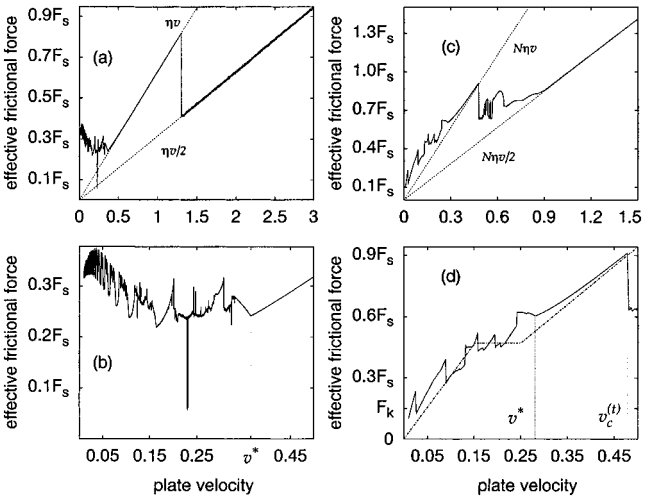

Figure 5. Effective frictional force acting on the top plate as a function of dimensionless plate velocity, $v = V/(b\omega)$. Dotted lines with slopes $N\eta$ and $N\eta/2$ are presented on parts a and c for reference. Parts a and b correspond to noninteracting particles, $\eta/m\omega = 0.1$. Parts c and d correspond to a chain and the dot−dashed line in the part d shows the smoothed force used for the approximate description according to eq 3; $N = 15$, $\eta/m\omega = 0.3$.

$$M\ddot{x} + F(\dot{x}) + K(x - vt) = 0 \tag{3}$$

where x is the position of the top plate and v is the stage velocity. Equation 3 and the effective force $F(\dot{x})$ can be shown[16] to be derived directly from the model discussed above. Under the assumption of separation of time scales, one can view the top plate as moving with a constant velocity, $\dot{x}$, and calculate $F(\dot{x})$ by averaging the potential and dissipative components of friction over the fast fluctuations of the system.[18] However, in order to simulate the motion of the top plate, the effective force should be supplemented by the static friction F_s and kinetic friction F_k, discussed above. Neither F_s nor F_k are included in the effective force found by time averaging. The kinetic friction force F_k could be found by calculating the average velocity of the top plate as a function of the driving force applied directly to the plate.[19,20]

Some general properties of the effective force $F(\dot{x})$ and the corresponding phases of the embedded chain can be obtained (see Figure 5), which do not strongly depend on the model:[16,18,21−23]

Property 1. For a given velocity $\dot{x}$, the frictional force per particle is always larger than $^1/_2\eta\dot{x}$. The minimal value $^1/_2\eta\dot{x}$ is obtained when the plate is moving with the rate faster than the characteristic intrinsic system rates ω and ω_{ch} (this resembles the widely observed thinning effect[8]). This friction law corresponds to the state where the embedded chain is decoupled from the plates, and is practically free, moving with a velocity of the center mass $v/2$. In this state the fluctuations in the particle velocities are small. The existence of a decoupled state should be model independent and is caused by the fact that in the frame moving with the center of mass; the periodic potentials act as forces with a high relative frequency. Because of the inertia the particles cannot follow these fast oscillations and behave as if the potential is absent.

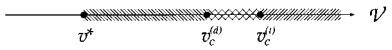

Figure 6. Characteristic velocities: v^* and $v_c^{(t)}$ are the lower and upper limits of the trapped sliding state; $v_c^{(d)}$ is the lower boundary of the region of stability of the decoupled sliding state.

In our model example the decoupled state becomes unstable below a certain value of the top plate velocity, which, for noninteracting particles, can be approximated by

$$v_c^{(d)} = \frac{2}{\pi}\omega b\sqrt{\sqrt{1+4\left(\frac{\eta}{m\omega}\right)^4} - 2\left(\frac{\eta}{m\omega}\right)^2} \tag{4}$$

Property 2. For $v < v_c^{(d)}$ the fluctuations of the particle velocity grow and the energy dissipation increases. At intermediate velocities, $v^* < v < v_c^{(t)}$, the chain is trapped by one of the plates and each particle performs small oscillations around the corresponding minimum of the particle−plate interaction potential. The frictional force corresponding to the trapped dynamic state, is

$$F(\dot{x}) = N\eta\dot{x} \tag{5}$$

where N is the number of particles in the chain.

Again the existence of an upper limit of sliding velocity $v_c^{(t)}$ above which a trapped state disappears, should not depend on the model. The reason is that, due to the dissipative forces between the particles and the plates, the trapped chain feels roughly a uniform force proportional the sliding velocity. If this force overcomes the depinning force (static friction, F_s) the chain becomes untrapped (decoupled). The limiting velocity is therefore

$$v_c^{(t)} = F_s/(\eta N) \tag{6}$$

The trapped state is stable only if the sliding velocity is larger than a critical v^*, which for noninteracting particles equals to

$$v^* = \frac{1}{\pi}\sqrt{\frac{3}{2}}\omega b\left[1 - 3\left(\frac{\eta}{m\omega}\right)^2 - O\left(\left(\frac{\eta}{m\omega}\right)^4\right)\right] \tag{7}$$

Here, as in the case of decoupled chain, the trapped state is destroyed for $v < v^*$ by the fluctuations of the particle velocity and v^* corresponds to a local minimum in $F(\dot{x})$. The presence of trapped liquid layers at moving surfaces is typical to many systems. We can speculate that already our simple chain picture gives the qualitative conditions for the existence of this phenomenon.

The different critical velocities discussed above are displayed in Figure 6 which correspond to transitions between different phases of motion.

One should note that if the stability intervals of trapped and decoupled states overlap ($v_c^{(t)} > v_c^{(d)}$) there is a bistability region and we expect hysteretic behavior.

Property 3. In the low velocity region, $v < v^*$, the center of mass of the chain moves again with the average velocity $v/2$, but its length strongly fluctuates. Here we find the following characteristic features of the frictional force which we smooth out to emphasize the general features: a "plateau" for $\dot{x}$ close to v^* and a positive slope of $F(\dot{x})$ for lower velocities. However, the width of the plateau, the slope of the smoothed $F(\dot{x})$ at small $\dot{x}$, and the limiting value for $\dot{x} \to 0$ depend on the internal parameters: on the ratio of the frequencies related to interparticle and particle−plate interactions, $\rho = (\omega_{ch}/\omega)^2$, and on the misfit δ of the substrate and chain periods. We find a finite effective friction at low velocities for small values of ρ and zero misfit (see Figure 5a). For noninteracting particles the value $F(v = 0)$ can be estimated as

$$F(v=0) \approx (4\pi)^{1/3}\left(\frac{\eta m}{\omega}\right)^{2/3} \tag{8}$$

In contrast, a "viscous-like" friction law, namely, $F(v = 0) = 0$, has been observed for $\rho \geq 1$ and nonzero misfit (see Figure 5c). These two limits correspond to the case where the particles perform microslips, $F(v = 0) \neq 0$, and to the case where the particles follow smoothly the top plate, $F(v = 0) = 0$, respectively. Similar effects have been also found in large scale molecular dynamics simulations.[12,15,24]

These considerations show that the properties of the velocity dependent friction $F(\dot{x})$ are strongly related to the dynamical nature of the embedded system.

How are the experimental results, found in SFA measurements, related to the properties of the effective frictional force and correspondingly to the dynamics of embedded molecular systems? As we have already discussed above one of the important experimental characteristics is a critical velocity v_c, which corresponds to a transition from stick−slip to sliding (Figure 2). However, the transition to smooth sliding, for which fluctuations are negligibly small, passes through a kinetic regime, where no sticking is observed but yet the motion is chaotic and the spring force displays large fluctuations. The smooth sliding itself is characterized by either a trapped state or by a decoupled state (the "thinning" phase), as discussed above. These make the determination of the critical velocity v_c, a quite delicate issue.

We obtain smooth sliding for $v > v^*$ where the trapped state becomes stable. However, stick−slip motion disappears at lower velocities $v < v^*$. The detailed features of the transition from stick−slip to sliding depend on the experimental conditions: overdamped or underdamped. In the overdamped regime, the stick−slip behavior should be observed for stage velocities for which

$$F(v) < F_k \tag{9}$$

This, together with eq 2, allow for a rough estimate of the critical velocity v_c if one approximates $F(\dot{x}) \propto \eta\dot{x}$. Namely, in terms of the static friction,

$$v_c \propto \sqrt{\frac{F_s b}{M}} \tag{10}$$

as proposed in.[13,14]

In the underdamped case[25]

$$v_c \sim \frac{F_s - F(0)}{\sqrt[4]{KM}\sqrt{2\pi F'(0)}} \tag{11}$$

This equation stems from the fact that under the underdamped condition the maximum velocity of the top plate is small (of the order of the stage velocity) and the stick−slip relaxation probes only the vicinity of $\dot{x} \approx 0$, where $F(\dot{x})$ can be approximated by a linear behavior, $F(\dot{x}) \approx F(0) + F'(0)\dot{x}$.

In contrast to v^*, which is a function of the internal parameters only, the critical velocity v_c is a function of both internal and external parameters. Equations 10 and 11 demonstrate that the critical velocities in overdamped and underdamped limits depend differently on the internal and external parameters. The amplitude of the stick−slip time patterns can be shown to be

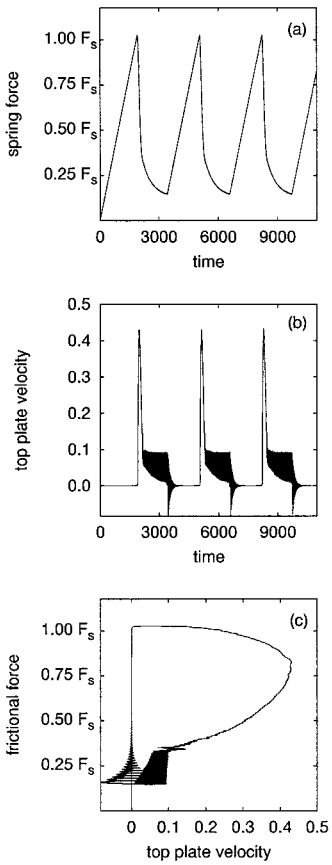

Figure 7. Time evolution of the spring force (a), top plate velocity (b), and instantaneous frictional force as a function of top plate velocity in the stick−slip regime (c). Dimensionless top plate velocity is presented in units ωb. $V/b\omega = 0.046$, $\epsilon = m/M = 1/120$, $N = 15$, $\delta = 0.05$, $\omega_{ch}/\omega = 1$, $\Omega/\omega = 0.015$.

$F_s - F_k$, under overdamped conditions, and $2(F_s - F(0))$ for the underdamped case. It should be noted that at least in our model system $F_k \neq F(0)$, contrary to what has been assumed previously.[10]

Our calculations performed for chains of finite length give nonzero values of static and kinetic friction forces even for the case where the chain and substrate structures are incommensurate. This leads to stick−slip motion at the macroscopic scale, in spite of the fact that under this conditions the effective force demonstrates viscous-like behavior, which corresponds to smooth motion of the embedded system at the microscopic scale. The existence of finite domains of coherent motion of a liquid under shear (chains of finite length in our model) could be a reason for stick−slip behavior which is common at macroscopic scale. This mechanism leads to stick−slip motion even in the case of incommensurability of the contacting surfaces.

The effective force calculated by averaging the potential and dissipative components of the friction appears valuable for describing the response of the top plate, and as we see later also in analyzing slip events. On the other hand, one can also obtain an instantaneous friction force directly from the time series of the stick−slip behavior, using the force balance eq 3. Because the effective force calculated above relies on the separation of time scales, it is averaged over the fast processes and therefore it is not necessary the same as the instantaneous force obtained directly from the time series. Figure 7 shows a typical stick−slip motion in the overdamped limit and its corresponding instantaneous frictional force versus the top plate velocity. This frictional force is clearly not a single-valued function of the top plate velocity as indeed observed experimentally in sheared granular materials.[17] It is clear that in this example the velocity is not sufficient to describe the dynamics of the system, and other variables are needed. Recently a model has been proposed in this direction.[26]

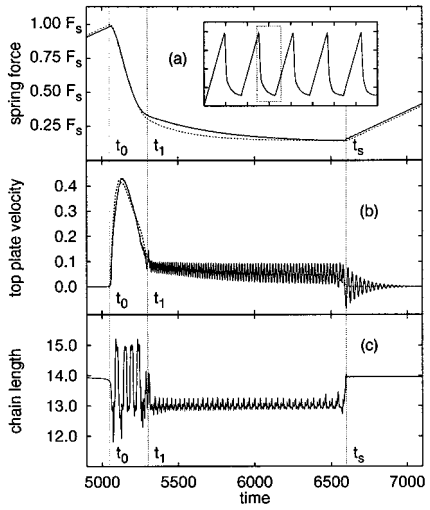

Figure 8. Time evolution of the spring force (a), top plate velocity (b), and length of the embedded chain (c), during slip relaxation. Solid lines are the results of simulations, dashed lines in parts a and b correspond to the effective force approximation. Inset shows a stick−slip time series with a window which indicates the time interval presented in Figs. a−c. Dimensionless stage velocity $V/(\omega b) = 0.046$; spring constant $\alpha = 0.015$.

Closer Look at Slip Events

We now focus on the properties of individual slip events and relate them to the previously discussed. It has been experimentally observed[10] that under overdamped conditions, "slip" relaxation manifests more than one characteristic time scale. Typically a sharp decrease at early times is followed by a tail of slow decay. Figure 8a displays the time evolution of the spring force during the slip motion which has been calculated for the chain embedded between two plates.[18] One clearly notices more than one time scale in the relaxation process. We divide the slip part into two intervals: $t_0 < t < t_1$ and $t_1 < t < t_s$, as marked in the figure. Following in time the velocity of the top plate (Figure 8b) reemphasizes the existence of two temporal behaviors. Figure 8b clearly demonstrates that in the time range $t_0 < t < t_1$ the velocity drops abruptly, and in the range $t_1 < t < t_s$ the velocity relaxes slowly toward the stage velocity. In the second time range the amplitude of the velocity oscillations is of order of the average velocity. The two behaviors observed for the spring force and the top plate velocity appear also in the properties of the chain. For instance, the chain length (Figure 8c) shows two distinctive regimes: strong fluctuations for $t_0 < t < t_1$ and quasiperiodic oscillations around a stretched state for $t_1 < t < t_s$.

Similar features of the top plate motion have been observed also in the case of the single particle model under overdamped conditions.[16] This is in contrast to underdamped results, where the slip time is shorter and slip motion is characterized by one type of behavior.

Basically, the relaxation pattern should depend on the maximum value of the velocity reached by the top plate. The latter increases with the decrease of the spring constant K. For our choice of parameters the maximum of the plate velocity lies in the range $v^* < v_{max} < v_c^{(t)}$. The relaxation process

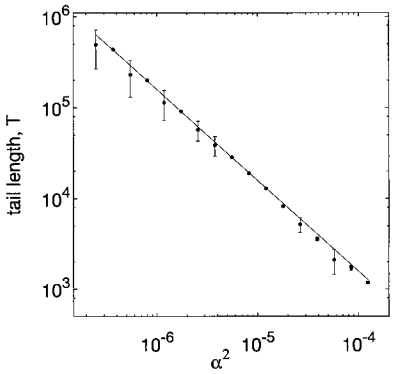

Figure 9. Duration of the slow part of slip relaxation as a function of dimensionless spring constant $\alpha^2 = K/(M\omega^2)$ plotted in double logarithmic axes. Error bars indicate a dispersion. The straight line with the slope -1 is the best fit to the results of simulations.

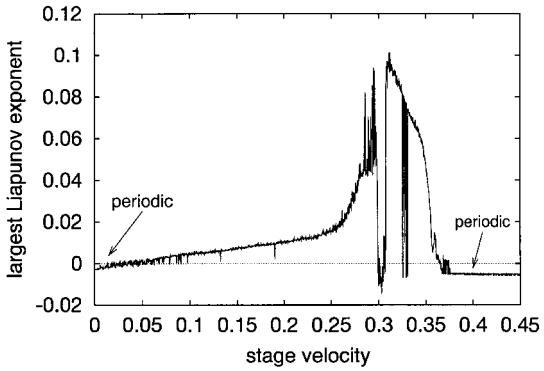

Figure 10. Velocity dependence of the largest Liapunov exponent.

spans velocities smaller than v_{max}, and therefore probes only those phases that correspond to $v < v_c^{(t)}$. Namely, only two regimes are to be expected. Indeed the initial part of the slip relaxation (or top plate velocity) results from the frictional force in the range $v^* < v < v_c^{(t)}$, and the longer time relaxation results from $F(v)$ in the range $v < v^*$. Both the time dependence and the amplitude of the slip relaxation predicted here are consistent with the experimentally observed behavior.[10]

For other choices of parameters, for which the maximum of the top plate velocity lies in the range $v > v_c^{(t)}$, the relaxation probes all three characteristic ranges of $F(v)$ leading to relaxation pattern with three distinct time scales.

The observed temporal behavior of the slip part depends on how broad is the probed range of the effective force $F(v)$. This, as mentioned, depends on v_{max}, which is determined by the experimentally chosen spring constant K. Thus, by changing the spring constant K one can control the experimentally observed relaxation pattern of the slip: one, two, or three types of relaxation. The weaker is K; the larger is the probed range of $F(v)$.

Another measurable feature that emerges from the current model is the K-dependence of the "slow" relaxation part, whose origin is in the low velocity effective force. Although this region of $F(v)$ is characterized by large fluctuations, we find that solving eq 3 for a smoothed $F(v)$ mimics well the slip relaxation presented in Figure 8a,b. The top plate velocity strongly oscillates at $t_1 < t < t_s$, providing "self-averaging" of the effective force. This is the reason why the smoothed force describes well the slip relaxation also in this time interval.

The use of eq 3 with the smoothed $F(v)$ shows that a positive slope of $F(v)$, such that $F'(v)^2 > 4KM$ is essential for the existence of the slow relaxation part. According to the coarse-grained picture the duration of this part of the slip $T = t_s - t_1$ should be proportional to $F'(v)/(2KM)$. The dependence of T on the spring constant K found in our simulations (see Figure 9) is in agreement with this conclusion. This result differs from the conclusion in the melting-freezing model,[26] where the duration of the slow relaxation interval is determined by the freezing rate τ^{-1} (a parameter not needed in our model) and does not depend of K. Thus the analysis of the slip relaxation could help to differentiate among various mechanisms of friction.

Summary and Future Directions

The effective frictional force appears to play a central role in understanding the dynamical properties of systems under shear and may therefore help in modifying and controlling frictional behavior. One should be able to deduce the effective frictional force directly from the experimental measurements, a direction which has been overlooked but which might be helpful in probing the nature of the embedded system.

Future investigations of various aspects of atomic scale friction should provide deeper insight to this long standing problem. In particular, we believe that relating the tribological approach described here to the traditional theological methods will help unify the views with different experimental results.

Another aspect which has been overlooked is the nonlinear nature of frictional dynamics. For a wide range of system parameters, we find that the motion of the top plate and the embedded molecules is chaotic. In order to provide a quantitative measure of the degree of stochasticity of the motion, we have calculated[16] the velocity dependence of the largest Liapunov exponent of the trajectories (see Figure 10). Any system with at least one positive exponent is defined to be chaotic.[27,28] The magnitude of the exponent reflects the time scale over which the system dynamics becomes unpredictable. It should be noted that Liapunov exponents can be extracted[29] from SFA measurements and provide additional information on the nature of the dynamics of the top plate. Chaos is clearly an intrinsic property of the confined liquids under shear, and it has been observed in systems which are largely free of inhomogeneities.[30]

A possible new direction has been recently proposed which allows to convert chaos into smooth sliding motion. From a practical point of view, one wishes to be able to control frictional forces so that the overal friction is reduced or enhanced, the chaotic regime is eliminated, and instead, smooth sliding is achieved. Such control can be of high technological importance for micromechanical devices, for instance, in computer disk drives, where the early stage of the motion and the stopping process, which exhibit chaotic stick−slip, poses a real problem.[31] Controlling frictional force has been traditionally approached by chemical means, namely, using lubricating liquids. A different approach is by controlling the system mechanically, for instance by modulating the normal load.[32,33] The goal is 2-fold: (a) to achieve smooth sliding at low driving velocities, which otherwise correspond to the stick−slip regime; (b) to decrease the frictional forces. This could lead to novel methods of reducing friction.[32,33]

Although we have discussed a relatively simple model, our conclusions are general and expected to underline the basics of nanotribology. This approach could be also applied to the description of dynamics of dry friction,[34,35] friction in granular materials,[17] and earthquakes.[36]

Acknowledgment. Financial support for this work by the Israel Science Foundation, administered by the Israel Academy

of Science and Humanities, by the German-Israeli Binational Science Foundation and by German−Israeli Project Cooperationis is gratefully acknowledged. M. R. acknowledges the support of the Alexander von Humboldt-Stiftung and the Estonian Science Foundation.

References and Notes

(1) Singer, I. L., Pollock, H. M., Eds. *Fundamentals of Friction, Series E: Applied Sciences*; NATO Advanced Sciences Institutes, Kluwer Academic Publishers: Dortrecht, 1992.
(2) Bhushan, B.; Israelachvili, J. N.; Landman, U. *Nature* **1995,** *374,* 607.
(3) Persson, B. N. J., Tosatti, E., Eds. In *Physics of Sliding Friction*; Kluwer Academic Publishers: Dordrecht, 1996.
(4) Langmuir **1996**,*12*.
(5) Bhushan, B., Ed. In *Micro/Nanotribology and Its Applications*, Series E: Applied Sciences 330, NATO Advanced Sciences Institutes; Kluwer Academic Publishers: Dortrecht, 1997.
(6) Persson, B. N. J. *Sliding Friction. Physical Principles and Applications*; Springer-Verlag: Berlin, 1998.
(7) Yoshizawa, H.; McGuiggan, P.; Israelachvili, J. *Science* **1993**, *259*, 1305.
(8) Hu, H.-W.; Carson, G. A.; Granick, S. *Phys. Rev. Lett.* **1991,** *66,* 2758.
(9) Klein, J.; Kumacheva, E. *Science* **1995**, *269,* 816.
(10) Berman, A. D.; Ducker, W. A.; Israelachvili, J. N. *Langmuir* **1996**, *12*, 4559.
(11) Yoshizawa, H.; Chen, Y. L.; Israelachvili, J. *J. Phys. Chem.* **1993**, *97,* 4128.
(12) Robbins, M. O.; Smith, E. D. *Langmuir* **1996**, *12,* 4543.
(13) Thompson, P. A.; Robbins, M. O. *Science* **1990,** *250,* 792.
(14) Thompson, P. A.; Robbins, M. O.; Grest, G. S. *Isr. J. Chem.* **1995**, *35,* 93.
(15) Bordarier, P.; Shoen, M.; Fuchs, A. H. *Phys. Rev. E* **1998**, *57*, 1621.
(16) Rozman, M. G.; Urbakh, M.; Klafter, J. *Phys. Rev. E* **1996**, *54*, 6485.
(17) Nasuno, S.; Kudrolli, A.; Gollub, J. P. *Phys. Rev. Lett.* **1997**, *79*, 949.
(18) Rozman, M. G.; Urbakh, M.; Klafter, J. *Europhys. Lett.* **1997**, *39*, 183.
(19) Strunz, T.; Elmer, F.-J. **1997**. Submitted for publication.
(20) Braiman, Y.; Family, F.; Hentschel, G. *Phys. Rev. B* **1996**, *55*, 5491.
(21) Rozman, M. G.; Urbakh, M.; Klafter, J. *Phys. Rev. Lett.* **1996**, *77*, 683.
(22) Braun, O.; Dauxois, T.; Peyrard, M. *Phys. Rev. B* **1997**, *56*, 4987.
(23) Roder, J.; Hammerberg, J. E.; Holian, B. L.; Bishop, A. R. *Phys. Rev. B* **1998**, *57*, 2759.
(24) Glosli, J. N.; McCleland, G. M. *Phys. Rev. Lett.* **1993**, *70*, 1960.
(25) Elmer, F.-J. *J. Phys. A: Math. Gen.* **1997**, *30*, 6057.
(26) Carlson, J. M.; Batista, A. A. *Phys. Rev. E* **1996**, *53*, 4153.
(27) Strogatz, S. H. *Nonlinear Dynamics and Chaos*; Addison-Wesley: Reading, MA, 1994.
(28) Wolf, A.; Swift, J. B.; Swinney, H. L.; Vastano, J. A. *Phys. D* **1985**, *16*, 285.
(29) Abarbanel, H. D. I.; Brown, R.; Sidorowich, J. L.; Tsimring, L. S. *Rev. Mod. Phys.* **1993**, *65*, 1331.
(30) Demirel, A. L.; Granick, S. *Phys. Rev. Lett.* **1996**, *77*, 4330.
(31) Mate, C. M.; Homola, A. M. In *Micro/Nanotribology and Its Applications*; Series E: Applied Sciences 330, NATO Advanced Sciences Institutes; Bhushan, B., Ed.; Kluwer Academic Publishers: Dortrecht, 1997; pp 647−661.
(32) Rozman, M. G.; Urbakh, M.; Klafter, J. *Phys. Rev. E* **1998**, *57*, 7340.
(33) Elmer, F.-J. *Phys. Rev. E* **1998**, *57*, R 4903.
(34) Johansen, A.; et al. *Phys. Rev. E* **1993**, *48*, 4779.
(35) Baumberger, T.; Heslot, F.; Perrin, B. *Nature* **1994**, *367*, 544.
(36) Carlson, J. M.; Langer, J. S.; Shaw, B. E. *Rev. Mod. Phys.* **1994**, *66*, 657.